

## Ultrasonic measurements of the bulk flow field in foams

Richard Nauber,<sup>1</sup> Lars Büttner,<sup>1</sup> Kerstin Eckert,<sup>2</sup> Jochen Fröhlich,<sup>3</sup> Jürgen Czarske,<sup>1</sup> and Sascha Heitkam<sup>2,\*</sup>

<sup>1</sup>*Faculty of Electrical and Computer Engineering, Laboratory for Measurement and Sensor System Technique, TU Dresden, 01069 Dresden, Germany*

<sup>2</sup>*Institute of Fluid Dynamics, Helmholtz-Zentrum Dresden-Rossendorf, Bautzner Landstrasse 400, 01328 Dresden, Germany*

<sup>3</sup>*Institute of Fluid Mechanics, TU Dresden, 01069 Dresden, Germany*



(Received 14 September 2017; published 23 January 2018)

The flow field of moving foams is relevant for basic research and for the optimization of industrial processes such as froth flotation. However, no adequate measurement technique exists for the local velocity distribution inside the foam bulk. We have investigated the ultrasound Doppler velocimetry (UDV), providing the first two-dimensional, non-invasive velocity measurement technique with an adequate spatial (10 mm) and temporal resolution (2.5 Hz) that is applicable to medium scale foam flows. The measurement object is dry aqueous foam flowing upward in a rectangular channel. An array of ultrasound transducers is mounted within the channel, sending pulses along the main flow axis, and receiving echoes from the foam bulk. This results in a temporally and spatially resolved, planar velocity field up to a measurement depth of 200 mm, which is approximately one order of magnitude larger than those of optical techniques. A comparison with optical reference measurements of the surface velocity of the foam allows to validate the UDV results. At 2.5 Hz frame rate an uncertainty below 15 percent and an axial spatial resolution better than 10 mm is found. Therefore, UDV is a suitable tool for monitoring of industrial processes as well as the scientific investigation of three-dimensional foam flows on medium scales.

DOI: [10.1103/PhysRevE.97.013113](https://doi.org/10.1103/PhysRevE.97.013113)

### I. INTRODUCTION

The measurement of the local velocity of flowing foam is a challenging task. Up to now, no technique is available that allows for the non-invasive, spatially and temporally resolved measurement of the foam velocity in the bulk of a foam sample.

Flowing foams play an important role in many industrial processes [1], such as the fractionation of surface active molecules and particles, food production, operation of multiphase-reactors, or the production of foam-filled insulation elements. In order to monitor the state of such processes and to control the foam movement, a direct, non-invasive measurement of the foam movement is desired.

Also from the point of view of fundamental research, the three-dimensional flow of liquid foam is sparsely investigated [2] because no adequate measurement technique exists. Many experiments rely on optical observation [3,4], where the penetration depth is limited by the refraction of light to a few bubble diameters [5]. Other experiments take into account integral values such as volumetric flows or pressure differences [6]. Recently, x-ray tomography has been applied to bubble rearrangement in liquid metal [7] and to rearrangement of foam around a moving sphere [8], but this technique requires high-energy radiation and is only applicable to measurement volumes of some millimeters. Magnetic resonance imaging (MRI) is also capable of measuring velocities inside complex fluids [9]. Rodts *et al.* [10] combined MRI with a rheometer to measure the velocity profile of a sheared foam. Drawbacks of this method are the high equipment costs and the very low

frame rate. Rodts *et al.* averaged their data over 90 s. Le Merrer *et al.* [11] used the laser scatter pattern to instantaneously detect bubble rearrangement in foam, but this technique does not deduce velocity information.

Our approach is the application of ultrasound Doppler velocimetry (UDV) to foam. In UDV, a sound pulse is sent through a foam sample, reflected by the liquid fluid interfaces, especially the plateau borders, and the echoes are recorded. From the time of flight and the speed of sound one can derive the position of the reflection target and from the Doppler phase shift its velocity. Figure 1 shows the operating principle. This technique has already been applied to flows of opaque liquids such as liquid metal [12–16], yielding spatially and temporally resolved velocity fields. However, liquid metal is a continuous fluid with low attenuation of the sound pulse. Reflection targets were well defined by tracer particles occurring naturally as, e.g., oxides in the melt.

Measurement of foam flow with UDV is more challenging, because foam absorbs the ultrasound very strongly [17] and the attenuation is not yet completely understood [18]. The deflection targets are soft, spacious, and variable air-liquid interfaces instead of particles. Furthermore, the speed of sound can vary widely in foams [17,18].

This paper demonstrates the applicability of UDV in liquid foam, evaluates the uncertainty of position and velocity, and identifies limitations. To that end, a model foam flow is designed and measured optically and with UDV simultaneously. A flat channel flow is chosen to enable the optical reference measurement. However, UDV is not restricted to thin channel flows. Penetration depths up to 20 cm are achieved, allowing for measurement inside thick channels. In fact, UDV is the first non-invasive velocity measurement technique for

\*S.Heitkam@hzdr.de

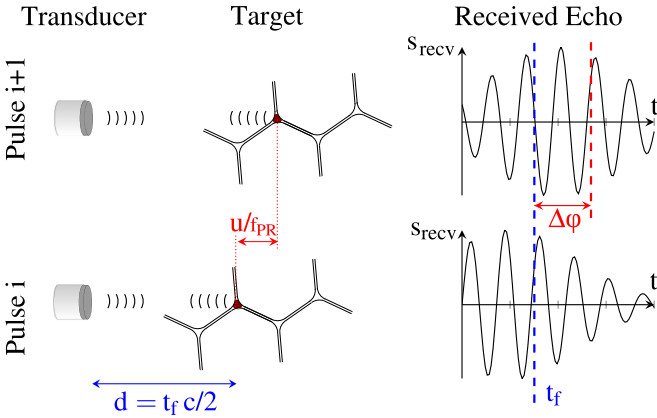


FIG. 1. Operating principle of ultrasound Doppler velocimetry in foam. The velocity  $u$  at a location  $d$  is estimated from the phase difference  $\Delta\phi$  of the reflected ultrasound wave over multiple pulses with an rate of  $f_{PR}$ .

three-dimensional foam flow, that offers reasonable spatial and temporal resolution for flow investigation and monitoring.

## II. MATERIALS AND METHODS

### A. Experimental setup

Measurements of the foam velocity are carried out in a fully transparent vertical foam channel made of acrylic glass. The channel is 1150 mm long and has a rectangular cross section (100 mm × 30 mm). At the bottom, compressed air is released at a flow rate of  $Q_L = 11 \text{ cm}^3/\text{min}$  through a steel pipe with 100 holes of 0.5 mm diameter, submerged in surfactant solution. This process generates a foam with bubbles of  $6 \pm 1 \text{ mm}$  diameter. The foam rises through the channel and is discharged side-wards at the top of the channel. In order to control the liquid fraction, a constant downward liquid flow through the channel can be introduced. To that end, surfactant solution is pumped through porous media in the upper part of the channel. This yields a liquid fraction constant over the vertical direction.

Different measurement techniques are applied simultaneously for referencing. The volumetric flow rates of compressed air and liquid are measured with two rotameters. The liquid fraction of the foam is detected by a conductivity measurement with four pairs of electrodes, located at the circumference of the cross section of the channel. Most importantly, optical observation yields the velocity distribution at one surface of the channel. Consecutive images are recorded with  $4\text{px}/\text{mm}@25 \text{ fps}$  under back-light illumination. The software package PIVLAB [19] is used to derive the foam velocity, applying a PIV correlation algorithm.

Since the exact rheological properties of the foam are not in the focus of this study, a cheap and easy to handle surfactant (German dish-washing soap ‘FIT’) has been employed. The concentration of  $5 \text{ g l}^{-1}$  is well above the critical micelle concentration of  $(2.0 \pm 0.5) \text{ g l}^{-1}$ , yielding a surface tension of  $(32 \pm 5) \text{ mN m}^{-1}$ . This is evaluated by pulling a lamella from the surface and measuring the corresponding force with a scale.

Two different geometries have been considered. The straight channel in Fig. 2 a is used to test the different

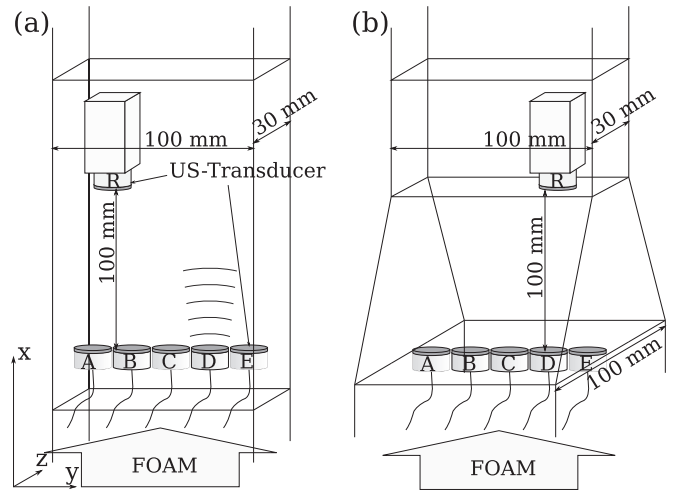


FIG. 2. Arrangement of US-transducer array (A...E) and reference transducer R in the foam channel (a) the straight channel and (b) nozzle.

parameters of the UDV postprocessing and to evaluate the attenuation and deflection properties of foam with different liquid fraction. Varying the volumetric flow of air, the upward foam velocities can be adjusted in order to validate the velocity measurement with UDV. The nozzle configuration in Fig. 2(b) is used to impose an inhomogeneous foam velocity field in order to demonstrate the spatial resolution of the UDV.

### B. Ultrasound flow instrumentation

The pulse-echo ultrasound Doppler velocimetry (UDV) allows spatially resolved flow measurements in opaque liquids [20]. We used a modular ultrasound research platform, the phased array ultrasound Doppler velocimeter (PAUDV) [21], which is an in-house development of the laboratory for measurement and sensor system techniques. Six identical circular piezoelectric ultrasound transducers with a center frequency  $f_0 = 175 \text{ kHz}$  (MCUSD19A175B11.5RS, Premier Farnell Ltd., Leeds, UK) are mounted in the foam channel. Five ultrasound transducers, labeled ‘A’ to ‘E’ form a linear array with a pitch of  $\Delta y = 20 \text{ mm} = 10.1\lambda$ . The sixth transducer, labeled ‘R’, is mounted upside-down above the array and serves as reference to deduce the speed of sound and the attenuation of the foam in between. Parameters of the UDV system are given in Table I. Sequentially, in the order A, B, C, D, E, R, one of the transducers transmits a pulse through the foam. The pulse propagates with the speed of sound  $c$  and is reflected by acoustic inhomogeneities, such as tracer particles or liquid/gas interfaces. After transmitting the pulse, the echo signal on all six transducers is recorded. However, due to slow-decaying reverberations of the transmitting element, the received echo signal of the transmitting element itself is overdriven for 0.3 ms. Therefore, only the echo signal from the other five, non-transmitting elements is processed. In Fig. 3 a typical echo signal and the corresponding spectrum is shown. The time of flight  $t_f$  of the echoes is directly related to the covered distance  $d$  by  $d = t_f c / 2$ . This allows for a spatial resolution along the beam propagation axis. Therefore the signals are sliced in 256 range gates of  $\Delta t = 3.2 \mu\text{s}$ ,

TABLE I. Specification of the ultrasound instrumentation.

transducer array	
elements	$n = 5$ cylindrical elements
element diameter	$D_{\text{ele}} = 19$ mm
element pitch	$\Delta y = 20$ mm = $10.1\lambda$
nominal center frequency	$f_0 = 175$ kHz
acoustic parameters	
speed of sound in air	$c_0 = 345$ m s <sup>-1</sup>
wavelength	$\lambda = 2.0$ mm
measurement parameters	
transmitted pulse signal	square wave $f_0 = 175$ kHz of $n_b = 5$ periods at $\pm 80$ V
received signal sampling rate	$f_{\text{samp}} = 625$ kHz
pulse repetition frequency	$f_{\text{PR}} = 250$ Hz
pulses for velocity estimation	$N_{\text{ep}} = 100$
measurement frame rate	$f_{\text{frame}} = 2.5$ Hz
maximum velocity at $c = c_0$	$u_{\text{max}} = 123$ mm s <sup>-1</sup>

representing different axial positions, which are processed separately [22].

The movement of the inhomogeneities with the velocity  $u$  along the beam axis causes a continuous shift  $\Delta\varphi$  in the phase of the subsequent echoes. This phase shift is determined and averaged for  $N_{\text{ep}}$  (emissions per profile) ultrasound pulse echoes with  $f_{\text{PR}}$  being the pulse repetition frequency [22]. From the average phase shift  $\overline{\Delta\varphi}$  the velocity of the moving inhomogeneity is determined by

$$u = \frac{c}{2} \frac{f_{\text{PR}} \overline{\Delta\varphi} / 2\pi}{f_0}. \quad (1)$$

As the phase shift  $\overline{\Delta\varphi}$  is ambiguous outside of  $\pm\pi$ , the measurable velocity lies in the range of  $\pm u_{\text{max}}$ , with [23]

$$u_{\text{max}} = \frac{c}{4} \frac{f_{\text{PR}}}{f_0}. \quad (2)$$

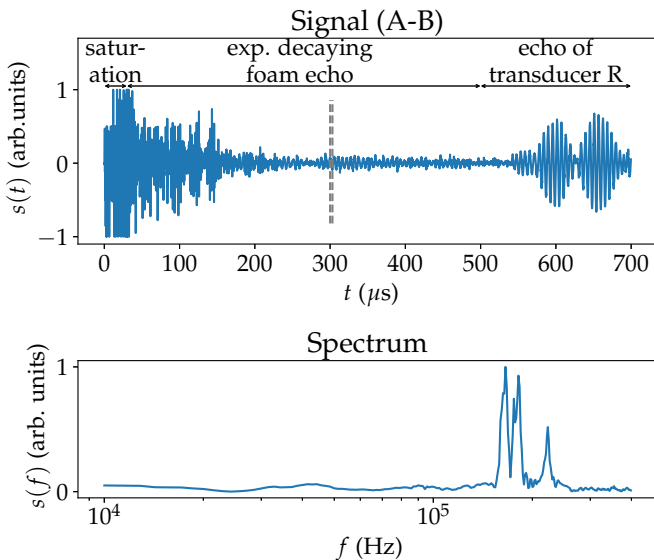


FIG. 3. Part of an echo signal received by transducer B after a single transmission of transducer A at  $t = 0$  and the corresponding spectrum. The dashed lines mark a range gate of  $\Delta t = 3.2$   $\mu$ s.

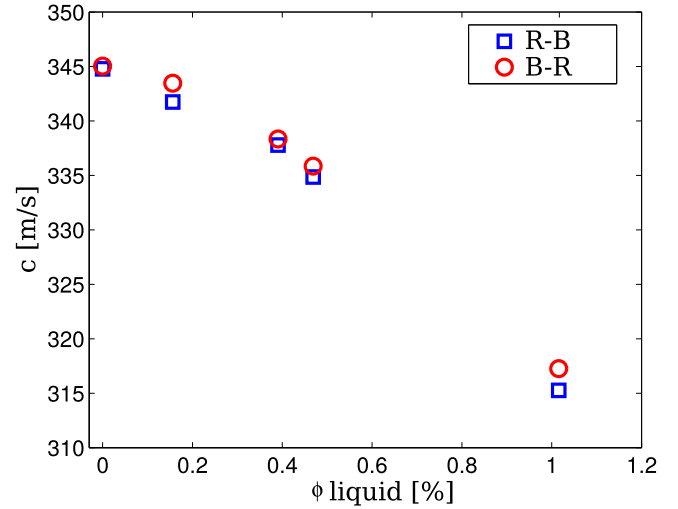


FIG. 4. Speed of sound in foam with different liquid fraction, derived from the time of flight between the reference transducer R and the transducer B and vice-versa. The value  $\phi = 0$  represents the empty channel.

This results in a maximum velocity of  $u_{\text{max}} = 123$  mm s<sup>-1</sup> for  $c = c_0$  and the parametrization given in Table I. The magnitude of all velocity measurements presented in this paper are well below this value.

### III. RESULTS

#### A. Straight channel

The speed of sound is an important parameter to analyze UDV measurements. It was reported to depend on the bubble size, the liquid fraction and the frequency [17,24]. For pure air at the ambient temperature of 22 °C, it equals  $c_0 = 345$  m s<sup>-1</sup>. For different liquid fractions  $c$  is measured by sending a pulse from transducer B to the reference transducer R and vice versa. The time of flight  $t_f$  is compared to that of the empty channel  $t_{f,0}$ , yielding  $c = c_0 t_{f,0} / t_f$ . The result is shown in Fig. 4. Small liquid content decreases the speed of sound, because it increases the overall density of the foam while having negligible influence on the compressibility. For the given bubble size and the relevant liquid fractions below 1%, the speed of sound changes about 10%.

The signal-to-noise ratio depends on the attenuation of the US in the foam. The signal intensity is tested by sending a pulse from one transducer and averaging the intensity of the signals recorded by the neighboring transducer over 0.3 ms. Figure 5 shows the intensity of the signal as a function of the liquid fraction of the foam. The signal intensity appears to be the best for foam with roughly  $\phi = 0.5\%$  liquid fraction. Presumably, higher liquid fractions cause too much attenuation while lower liquid fractions do not backscatter enough intensity. Suitable UDV measurements were found possible only for liquid fractions below 1% with bubble diameters of  $D_b \approx 6$  mm =  $3\lambda$ . We also tested foam with  $D_b \approx 0.5$  mm =  $\frac{1}{4}\lambda$ , but we did not receive analyzable echoes, presumably due to the high liquid holdup in fine foam.

To access the uncertainty of the velocity measurement, a constant air flow rate of 11 cm<sup>3</sup>/s has been applied,

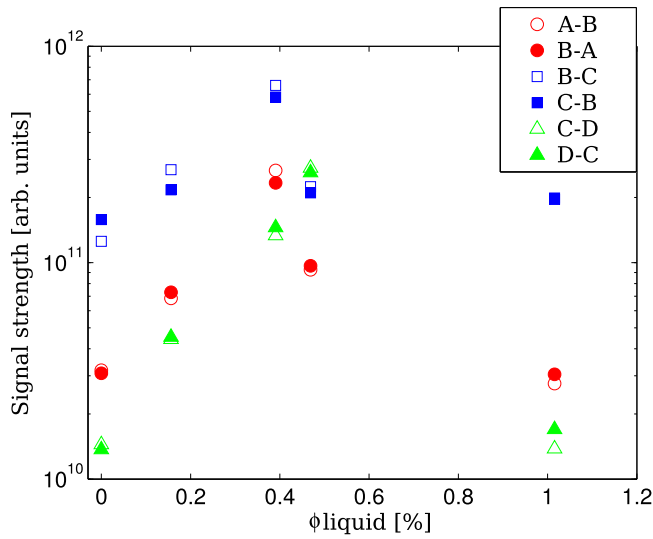


FIG. 5. Signal intensity as a function of the foam liquid fraction. One transducer sends a pulse and the signal recorded by neighboring transducer is integrated over 0.3ms. The value  $\phi = 0$  represents the empty channel. The noise level of the measurement setup is approximated as  $5 \times 10^8$  [arb. units].

yielding foam with a liquid fraction of  $\phi = (0.65 \pm 0.05)\%$ . The resulting velocity field at the surface, measured with optical image correlation, is shown in Fig. 6. This serves as a reference for the bulk velocity when the velocity gradient in  $z$ -direction is negligible. Simultaneously, UDV measurements are carried out with the transducers A–E. Figure 7 shows the resulting signal intensities and measured velocities, respectively.

In general, the velocities correspond well with the optical reference measurement. The constant mean velocity is well represented. In the region below 10 mm distance from the transducers, nonphysical velocity fluctuations are measured,

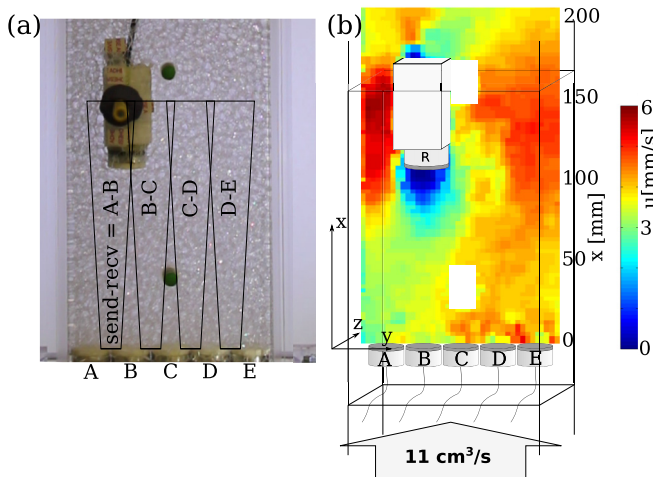


FIG. 6. Foam flow measurement in the straight channel: (a) picture of the applied foam flow, indicating the measurement volumes, (b) resulting vertical velocity distribution of the foam for  $11 \text{ cm}^3/\text{s}$ , measured with optical image correlation. The white spots above transducer C are caused by optical blockage.

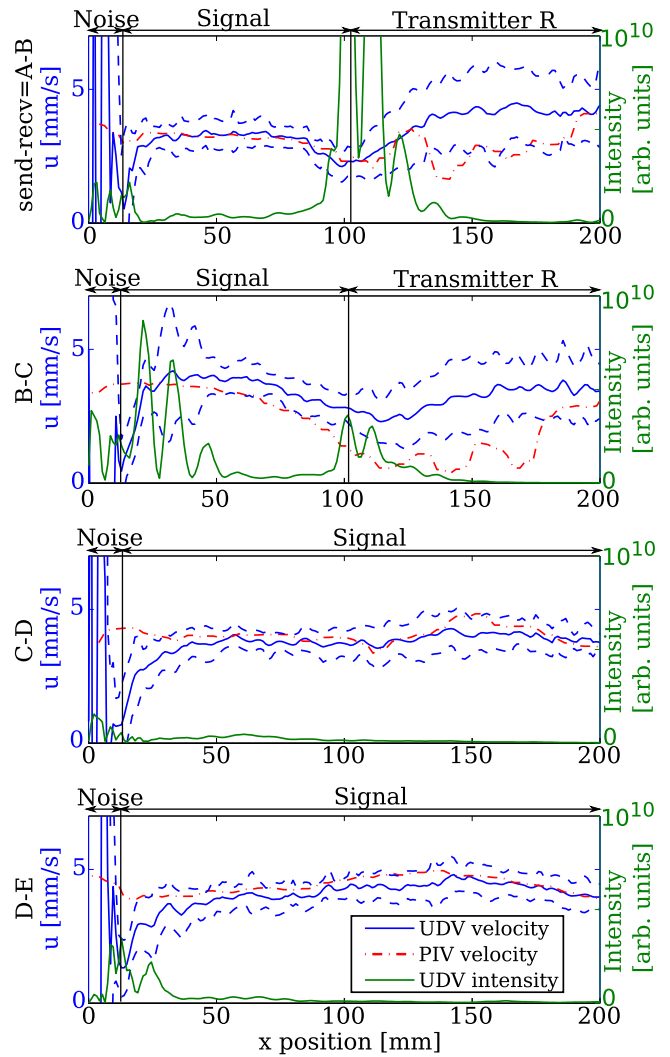


FIG. 7. Vertical velocity distribution in the straight channel, measured by UDV. Each plot corresponds to one measurement region in Fig. 6. The dashed lines mark the standard deviation of the measurement and the solid green line the corresponding signal strength. The dash-dotted red line gives the expected distribution, derived from the optical measurement in Fig. 6.

likely resulting from acoustic coupling of sending and receiving transducers. Between 10 mm and 30 mm, the flow accelerates, closing the wake of the transducers. Between 30 mm and 100 mm, a velocity plateau is measured, reflecting the homogeneous velocity distribution in the channel. In this region, deviations from the optical reference measurement in Fig. 6 are below 15%. With increasing distance, the signal intensity drops and for distances larger than 200 mm the measurement becomes unreliable. At a distance of 100 mm, an intensity peak and a velocity minimum is prominent in the lines A-B and B-C. This corresponds to the position of the reference transducer R (visible in Fig. 6), reflecting the US pulse. The measured velocity is reduced but not zero, because the UDV averages over a certain transversal region, due to the finite beam width.

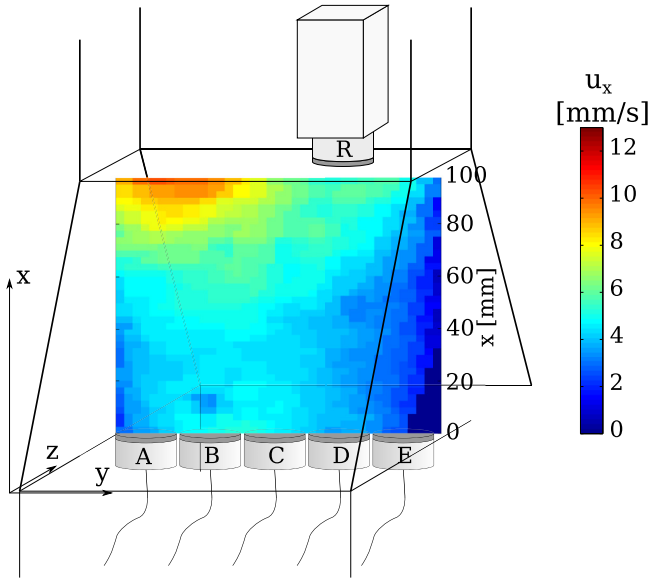


FIG. 8. Vertical velocity distribution in the channel with decreasing cross section, derived from image correlation.

### B. Nozzle

In order to test the axial resolution of the sensor, an inhomogeneous velocity field is investigated. The foam with a liquid fraction of  $\phi = (0.55 \pm 0.02)\%$  flows upward through a channel narrowing from  $100 \times 100 \text{ mm}^2$  to  $100 \times 30 \text{ mm}^2$  cross section. Due to conservation of volume, this causes an acceleration to 3.3 times the inlet speed. The velocity distribution in the channel is given in Fig. 8.

Figure 9 shows the resulting signal intensity and the measured velocity, respectively. The velocity profile, resulting from the optical reference measurement, is plotted in Fig. 9 as well. At the transition to the straight channel a flange is present, blocking the optical measurement.

UDV and optical measurement values corresponds well. The UDV can detect the increase of the velocity and the length of the nozzle. Again, at 100 mm distance, the reference transducer is mounted (see Fig. 2), blocking the flow and causing an intensity peak in the data of C-D and D-E. In order to derive an upper limit for the spatial resolution in beam direction, a perfect velocity measurement is assumed. In this case, the standard deviation of the velocity  $\sigma_u$  would arise completely from the standard deviation of the position  $\sigma_x$ , yielding

$$\sigma_u = \sigma_x \frac{\partial u}{\partial x}. \quad (3)$$

With the given velocity slope of approximately  $0.1 \text{ s}^{-1}$  and the standard deviation of the velocity of  $1 \text{ mm s}^{-1}$  this results in a axial resolution better than 10 mm.

The lateral resolution is estimated from the fact that the B-C measurement does not show an intensity peak from the edge of transducer R. As they are separated 20 mm laterally, a lateral resolution better than 40 mm at a measurement depth of 100 mm can be deduced.

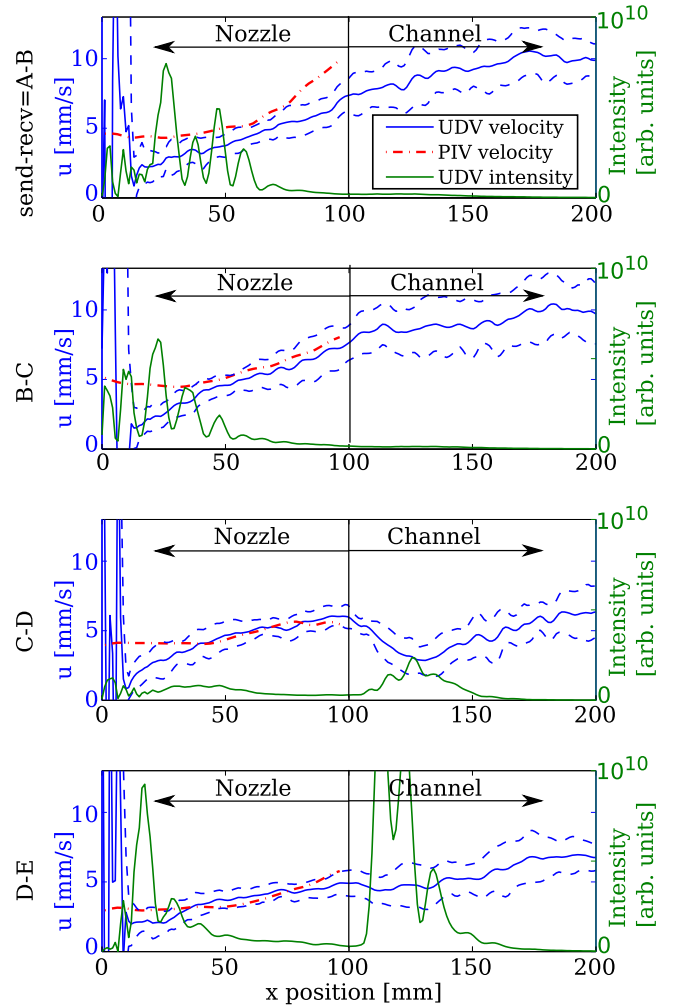


FIG. 9. Vertical velocity distribution in a nozzle, measured by UDV. The dashed lines mark the standard deviation of the measurement and the green line the corresponding signal strength. The dash-dotted red line gives the expected distribution, derived from the optical measurement in Fig. 8.

## IV. DISCUSSION

Our results demonstrate that the application of UDV to flowing foam is a promising technique. A velocity uncertainty below 15% and a spatial resolutions better than 10 mm in axial and 40 mm in lateral direction has been achieved. The temporal resolution results from the pulse repetition frequency and the number of pulses analyzed to derive the Doppler frequency shift. In our case, this results in 2.5 Hz frame rate.

Even though UDV measurement in general works, some limitations exist. Signal strength is crucial in the measurements. Due to the high attenuation of wet foam, the experiments are limited to very dry foam below 1% liquid fraction. However, in the absence of continuous drainage feed from top, water-based foam dries out very fast. Therefore, such low liquid fractions could be of high relevance, e.g., in the froth zone of flotation cells.

An approach to increase the US echo intensity could be varying the US frequency, as the attenuation strongly depends

on it [17]. However, the dependency of the spatial resolution and the maximum measurable velocity of the UDV method has to be taken into account. Another approach for higher signal intensity would be beam-forming [25] based the phased-array principle. This allows to focus ultrasound at an arbitrary position with a significantly increased sound intensity. Hence, higher signal-to-noise ratios, reduced measurement uncertainty and deeper measurement depth can be expected, as well a significantly improved lateral resolution. The phased array technique requires an US transducer array with an element pitch smaller than half the wavelength and tunable per-channel phase delays, which can be provided by the PAUDV system.

In the present setup, the transducers are mounted within the foam channel, influencing the foam flow. However, the UDV technique itself is non-invasive. With some effort the transducers could be flush mounted to the wall, especially if the foam flows around an object or a corner. Usage of the phased-array technique could also resolve the wall-parallel velocity [21].

In conclusion, we successfully measured the bulk velocity of liquid foam, using the UDV technique. To the best of our knowledge, this is the first spatially and temporally resolved, non-invasive measurement technique that could be applied to measure the foam velocity distribution in a duct or in a flotation cell. It has low equipment costs and does not use ionizing rays. Thus, UDV could be highly relevant for further investigations on foam flow. Additionally, US transducers are very robust and not as prone to staining as optical methods. Thus, UDV might also be relevant for industrial applications, e.g., the monitoring of froth movement.

#### ACKNOWLEDGMENTS

The support of the Max-Buchner-Forschungsstiftung (MBFSt-3534) and of the Deutsche Forschungsgesellschaft (HE 7529/1-1 and partially BU 2241/2-1) is gratefully acknowledged. We also thank our colleagues from NetFlot (KIC RawMaterials Project No. 15062, infrastructure network “Modelling of flotation processes”) for valuable discussions.

- 
- [1] P. Stevenson, *Foam Engineering: Fundamentals and Applications* (John Wiley & Sons, New York, 2012).
  - [2] S. Cohen-Addad, R. Höhler, and O. Pitois, *Annu. Rev. Fluid Mech.* **45**, 241 (2013).
  - [3] A. Bronfort and H. Caps, *Colloids Surf. A* **473**, 141 (2015).
  - [4] B. Dollet and C. Bocher, *Eur. Phys. J. E* **38**, 1 (2015).
  - [5] A. van der Net, L. Blondel, A. Saugey, and W. Drenckhan, *Colloids Surf. A* **309**, 159 (2007).
  - [6] B. Herzhaft, S. Kakadjian, and M. Moan, *Colloids Surf. A* **263**, 153 (2005).
  - [7] F. García-Moreno, P. Kamm, T. Neu, K. Heim, A. Rack, and J. Banhart, *Colloids Surf. A* **534**, 78 (2017).
  - [8] C. Raufaste, B. Dollet, K. Mader, S. Santucci, and R. Mokso, *Europhys. Lett.* **111**, 38004 (2015).
  - [9] D. Bonn, S. Rodts, M. Groenink, S. Rafai, N. Shahidzadeh-Bonn, and P. Coussot, *Annu. Rev. Fluid Mech.* **40**, 209 (2008).
  - [10] S. Rodts, J. Baudez, and P. Coussot, *Europhys. Lett.* **69**, 636 (2005).
  - [11] M. Le Merrer, S. Cohen-Addad, and R. Höhler, *Phys. Rev. Lett.* **108**, 188301 (2012).
  - [12] S. Eckert and G. Gerbeth, *Exp. Fluids* **32**, 542 (2002).
  - [13] V. Galindo, R. Nauber, D. Rübiger, S. Franke, H. Beyer, L. Büttner, J. Czarske, and S. Eckert, *Phys. Fluids* **29**, 114104 (2017).
  - [14] R. Nauber, M. Burger, L. Büttner, S. Franke, D. Rübiger, S. Eckert, and J. Czarske, *Eur. Phys. J. Spec. Top.* **220**, 43 (2013).
  - [15] L. Büttner, R. Nauber, M. Burger, D. Rübiger, S. Franke, S. Eckert, and J. Czarske, *Meas. Sci. Technol.* **24**, 055302 (2013).
  - [16] R. Nauber, N. Thieme, H. Radner, H. Beyer, L. Büttner, K. Dadzis, O. Pätzold, and J. Czarske, *Flow Meas. Instrum.* **48**, 59 (2016).
  - [17] J. Pierre, R.-M. Guillermic, F. Elias, W. Drenckhan, and V. Leroy, *Eur. Phys. J. E* **36**, 113 (2013).
  - [18] J. Pierre, B. Giraudet, P. Chasle, B. Dollet, and A. Saint-Jalmes, *Phys. Rev. E* **91**, 042311 (2015).
  - [19] W. Thielicke and E. J. Stamhuis, *J. Open Res. Softw.* **2**, e30 (2014).
  - [20] Y. Takeda, *Nucl. Eng. Des.* **126**, 277 (1991).
  - [21] K. Mäder, R. Nauber, V. Galindo, H. Beyer, L. Büttner, S. Eckert, and J. Czarske, *IEEE Trans. Ultrason. Ferroelectr. Freq. Control* **64**, 1327 (2017).
  - [22] C. Kasai, K. Namekawa, A. Koyano, and R. Omoto, *IEEE Trans. Sonics Ultrason.* **32**, 458 (1985).
  - [23] W. R. Hedrick, D. L. Hykes, and D. E. Starchman, *Ultrasound Physics and Instrumentation* (Elsevier, Mosby, St. Louis, 2005).
  - [24] J. Pierre, B. Dollet, and V. Leroy, *Phys. Rev. Lett.* **112**, 148307 (2014).
  - [25] O. T. von Ramm and F. L. Thurstone, *Circulation* **53**, 258 (1976).